

Spatial patterns of the Brusselator model with asymmetric Lévy diffusion

Hongwei Yin(尹洪位), Shangtao Yang(杨尚涛), Xiaoqing Wen(文小庆), Haohua Wang(王浩华), and Shufen Yang(杨淑芬)

Citation: Chin. Phys. B, 2024, 33 (**11**): 110202. DOI: 10.1088/1674-1056/ad74e5
Journal homepage: http://cpb.iphy.ac.cn; http://iopscience.iop.org/cpb

What follows is a list of articles you may be interested in

On fractional discrete financial system: Bifurcation, chaos, and control

Louiza Diabi, Adel Ouannas, Amel Hioual, Shaher Momani, and Abderrahmane Abbes
Chin. Phys. B, 2024, 33 (**10**): 100201. DOI: 10.1088/1674-1056/ad5d96

Prediction of collapse process and tipping points for mutualistic and competitive networks with *k*-core method

Dongli Duan(段东立), Feifei Bi(毕菲菲), Sifan Li(李思凡), Chengxing Wu(吴成星), Changchun Lv(吕长春), and Zhiqiang Cai(蔡志强)
Chin. Phys. B, 2024, 33 (**5**): 050201. DOI: 10.1088/1674-1056/ad3341

Exact solutions of a time-fractional modified KdV equation via bifurcation analysis

Min-Yuan Liu(刘敏远), Hui Xu(许慧), and Zeng-Gui Wang(王增桂)
Chin. Phys. B, 2023, 32 (**12**): 120204. DOI: 10.1088/1674-1056/acf9e8

Turing pattern selection for a plant-wrack model with cross-diffusion

Ying Sun(孙颖), Jinliang Wang(王进良), You Li(李由), Nan Jiang(江南), and Juandi Xia(夏娟迪)
Chin. Phys. B, 2023, 32 (**9**): 090203. DOI: 10.1088/1674-1056/acac13

An incommensurate fractional discrete macroeconomic system: Bifurcation, chaos, and complexity

Abderrahmane Abbes, Adel Ouannas, and Nabil Shawagfeh
Chin. Phys. B, 2023, 32 (**3**): 030203. DOI: 10.1088/1674-1056/ac7296

Spatial patterns of the Brusselator model with asymmetric Lévy diffusion

Hongwei Yin(尹洪位)[1,†], Shangtao Yang(杨尚涛)[1], Xiaoqing Wen(文小庆)[1], Haohua Wang(王浩华)[2], and Shufen Yang(杨淑芬)[3]

[1] *School of Mathematics and Statistics, Xuzhou University of Technology, Xuzhou* 221111, *China*
[2] *School of Mathematics and Statistics, Hainan University, Haikou* 570228, *China*
[3] *Jiangxi Institute of Applied Science and Technology, Nanchang* 330100, *China*

(Received 11 June 2024; revised manuscript received 25 August 2024; accepted manuscript online 29 August 2024)

The formation of spatial patterns is an important issue in reaction–diffusion systems. Previous studies have mainly focused on the spatial patterns in reaction–diffusion models equipped with symmetric diffusion (such as normal or fractional Laplace diffusion), namely, assuming that spatial environments of the systems are homogeneous. However, the complexity and heterogeneity of spatial environments of biochemical reactions *in vivo* can lead to asymmetric diffusion of reactants. Naturally, there arises an open question of how the asymmetric diffusion affects dynamical behaviors of biochemical reaction systems. To answer this, we build a general asymmetric Lévy diffusion model based on the theory of a continuous time random walk. In addition, we investigate the two-species Brusselator model with asymmetric Lévy diffusion, and obtain a general condition for the formation of Turing and wave patterns. More interestingly, we find that even though the Brusselator model with symmetric diffusion cannot produce steady spatial patterns for some parameters, the asymmetry of Lévy diffusion for this model can produce wave patterns. This is different from the previous result that wave instability requires at least a three-species model. In addition, the asymmetry of Lévy diffusion can significantly affect the amplitude and frequency of the spatial patterns. Our results enrich our knowledge of the mechanisms of pattern formation.

Keywords: asymmetric Lévy diffusion, Turing and wave patterns, Brusselator model

PACS: 02.30.Oz, 45.70.Qj **DOI:** 10.1088/1674-1056/ad74e5

1. Introduction

Since the pioneering work of Alan Turing proposed a reaction–diffusion chemical model (called the Turing model),[1] Turing patterns, a type of organized heterogeneous macroscopic structure, began to be widely investigated in chemical reaction systems[2] to physical systems[3] and ecological systems,[4] and are still a hot topic in many fields, such as epidemiology,[5] developmental biology[6] and so on. In all these works, it is implied that the critical eigenvalue of Turing bifurcation is real. However, wave bifurcation, induced by a complex critical eigenvalue, has received less attention. Korvasová *et al* in Ref. [7] pointed out that wave instability requires at least a three-species model.

Although research on Turing patterns has been going on for decades, most of the reaction–diffusion systems so far are modeled by adding normal and cross-diffusion terms into the original ODE models,[8] namely, for a one-step jump of reactants both the waiting time distribution and jump distance distribution have finite moments. In the real world, the complexity of reactants' jump processes and the anisotropy of spatial environments, such as congestion between reactants and transporter proteins helping signaling molecules to rapidly spread to other positions in cells,[9] can affect the diffusion of reactants, leading to anomalous diffusion rather than normal diffusion. Unlike normal diffusion, which is characterized by the dependence of the mean square displacement of the diffusing particles on time $\langle(\Delta x)^2\rangle \sim t$, anomalous diffusion is characterized by $\langle(\Delta x)^2\rangle \sim t^{\alpha}$. This diffusion with $\alpha > 1$, faster than normal diffusion, is called superdiffusion, and that with $0 < \alpha < 1$, slower than the normal diffusion, is called subdiffusion.[10] Dynamical models with superdiffusion are constructed by replacing the Laplace operator Δ by the fractional Laplace operator $-(-\Delta)^{\alpha/2}$, $0 < \alpha < 2$. In particular, when $\alpha = 2$ fractional Laplace diffusion can reproduce normal diffusion. Compared with models with normal diffusion, Turing patterns of models with fractional Laplace diffusion have some distinct differences[11,12] and are explored by the same methods, such as weakly nonlinear analysis and analysis of the amplitude equations.[13,15,16]

An alternative theoretical framework characterizing anomalous diffusions describes the reactants' walk processes by continuous time random walks (CTRWs)[17] in a way to make the inter-event time continuous and fluctuating; this has been known for over 50 years.[18] Based on this framework, Lévy diffusion, an important type of anomalous diffusion,[14] is specifically stated through a probability density function (PDF) with variance of the diverging jump length, which is a joint PDF of the jump length and the waiting time for one jumping event.[19] So far, most current works focusing on Lévy diffusion assume that the PDF of the reactants' jump length is symmetric, since the environments of reaction sys-

†Corresponding author. E-mail: hongwei-yin@hotmail.com

© 2024 Chinese Physical Society and IOP Publishing Ltd

tems are homogeneous, resulting in the Lévy diffusion operators being symmetric and expressed by the fractional Laplace operators. The real environments are usually heterogeneous or nonidentical, leading to the result that reactants have different lengths for each jump in different spatial directions, and implying that asymmetric diffusion of reactants occurs. The PDF of the jump length for each jump event cannot be symmetric.

As far as we know, there has been little research on the spatial patterns of some systems with asymmetric Lévy diffusion. How the asymmetry of Lévy diffusion affects the spatial patterns remains unclear. In order to answer this problem, this paper will first establish a generalized model with an asymmetric Lévy diffusion operator based on the CTRW theory,[17,20,21] and then obtain a general Brusselator model with asymmetric Lévy diffusion. It is well known that the Brusselator model, proposed by Ilya Prigogine and his collaborators,[22] is a classical model of an autocatalytic reaction and possesses rich dynamic behaviors.[23] Through our research, we obtain a general condition for producing Turing and wave patterns for the Brusselator model with asymmetric Lévy diffusion. More interestingly, we find that for a certain set of parameters the Brusselator model with asymmetric diffusion can produce wave patterns, but spatial patterns cannot form for this model with symmetric diffusion (such as normal and fractional Laplace diffusion). This implies that the asymmetry of Lévy diffusion can form spatial patterns, which is different from the previous result in Ref. [7] that wave instability requires at least a three-species model.

This paper is organized as follows. In Section 2, a general model with asymmetric Lévy diffusion is built based on CTRW theory. In Section 3, we theoretically and numerically study the Brusselator model with asymmetric Lévy diffusion, obtaining the condition for forming Turing patterns, and find the interesting result that the asymmetry of Lévy diffusion can produce Turing patterns even though the Brusselator model with symmetric diffusion for a certain parameter regime cannot produce spatial patterns. Finally, a brief conclusion is given.

2. The asymmetric Lévy diffusion model

First, we will use CTRW theory to produce a generalized model with asymmetric diffusion. For convenience, here we consider the CTRW of only a type of particle in one-dimensional space. Our following model is easy to improve for multiple kinds of particles in two- or three-dimensional space. We define $c(x,t)$ to be a concentration of particles at position x and time t and assume a function $\Psi(x,t)$ to be the joint probability distribution that the particles jump a distance x after waiting a time t in a single jumping step, where x is a scalar or vector. If x is a vector, it represents a jump length vector in two- or three-dimensional space. Associated with this probability distribution are the usual waiting time probability density (WTPD), $w(t)=\int\Psi(x,t)\,\mathrm{d}x$, and the probability density for the jump length (JLPD) in a singe-step jump, $\chi(x)=\int_0^\infty\Psi(x,t)\,\mathrm{d}t$. The forms of these two probability densities decide the normal or anomalous (subdiffusive, superdiffusive or Lévy diffusive) character of the particles' diffusion.[24] Then, the renewal equation for the particles is obtained as

$$\begin{aligned}c(x,t) &= \Phi(t)c(x,0)+\int_{\mathbb{R}}\int_0^t\Psi(x-x',t-t')c(x',t')\,\mathrm{d}t'\,\mathrm{d}x'\\ &\quad+\int_0^t\Phi(t-t')f(x,t')\,\mathrm{d}t',\end{aligned}\tag{1}$$

where $c(x,0)$ represents the particles' initial concentration and $\Phi(t)$ denotes the probability of a waiting time longer than t, $\Phi(t)=1-\int_0^t w(x')\,\mathrm{d}x'$. The heuristic interpretation of Eq. (1) is that the first term on the right-hand side of Eq. (1) describes the concentration of the particles not jumping from x over time t; the second term describes the concentration of the particles reaching position x at time t after jumping from position x' and time t'; and the third term describes the concentration of the particles' reaction, for example degradation or production at position x and time t' but still retained after the time interval $t-t'$. If the reacting particles are among the walkers, then the reaction function $f(x,t)$ is replaced with $f[c(x,t)]$. We assume that WTPD $w(t)$ and JLPD $\chi(x)$ are independent of each other, and then $\Psi(x,t)=w(t)\chi(x)$. If the WTPD $w(t)$ has a fat tail, resulting in its first moment being infinite (or divergent), then the PDF $\Psi(x,t)$ corresponds to subdiffusion, and if the second moment of the JLPD is diverging, then the PDF $\Psi(x,t)$ corresponds to Lévy diffusion. However, if the first moment of the WTPD and the second moment of the JLPD are both finite, the PDF $\Psi(x,t)$ corresponds to Gaussian diffusion in the long-time limit.[17]

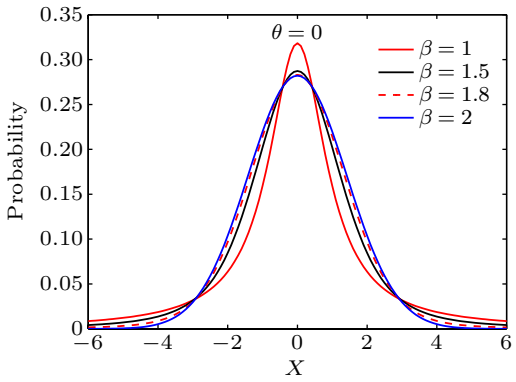


Fig. 1. The Lévy probability density is symmetric in the case of $\theta=0$.

In order to study asymmetric Lévy diffusion, we need to introduce the JLPD $\chi(x)$ with an Lévy strictly stable density function, which possesses infinite jump length variance. Its characteristic function is given by

$$\widehat{\chi}(k)=\exp\left(-\sigma^\beta\eta_\theta^\beta(k)\right),\tag{2}$$

where $\eta_\theta^\beta(k) = |k|^\beta \exp(\mathrm{i}(\mathrm{sign}(k))\theta\pi/2)$.[25] The parameter β $(0 < \beta \leq 2)$ is an index that characterizes the stability of a Lévy distribution. If the parameter β is less than 2, then the Lévy distribution is equipped with a long tail (see Fig. 1). The parameter θ, with $|\theta| \leq \min\{\beta, 2-\beta\}$, represents the skewness that describes the degree of asymmetry of the distribution (see Fig. 2), wherein the Lévy distribution is symmetric about the origin for $\theta = 0$ but asymmetric about the origin for $\theta \neq 0$. $\Gamma(\cdot)$ is the gamma function. On the other hand, the Laplace and Fourier transforms of w and χ have the following approximations:

$$\widetilde{w}(s) \sim 1 - \tau^\alpha s^\alpha + \mathcal{O}(\tau^2), \tag{3a}$$

$$\widehat{\chi}(k) \sim 1 - \sigma^\beta \eta_\theta^\beta(k) + \mathcal{O}(k^4). \tag{3b}$$

For the different parameters α, θ and β, the PDF $\Psi(x,t)$ corresponds to the different types of diffusions (see Ref. [17] for details). In Eq. (3), the memory (or a non-Markov process) of the particles' jumping event can be mathematically described by setting $\alpha \in (0,1)$. When $\alpha = 1$, the waiting time of the particles' jumping event follows an exponential distribution, that is, it is memoryless (or a Markov process). For Eq. (1), we apply the spatial Fourier transform with respect to the space variable x and the Laplace transform with respect to the time variable t, obtaining

$$\begin{aligned} s\widehat{\widetilde{c}}(k,s) \;=\; & (1-\widetilde{w}(s))\widehat{c}(k,0) + s\widetilde{w}(s)\widehat{\chi}(k)\widehat{\widetilde{c}}(k,s) \\ & + (1-\widetilde{w}(s))\widehat{f}(k,s). \end{aligned} \tag{4}$$

Substituting Eq. (3) into Eq. (4), simplifying this equation and retaining only a leading order, one can obtain

$$\begin{aligned} s^\alpha \widehat{\widetilde{c}}(k,s) \;=\; & s^{\alpha-1}\widehat{c}(k,0) - \frac{\sigma^\beta \eta_\theta^\beta(k)}{\tau^\alpha}\widehat{\widetilde{c}}(k,s) \\ & + s^{\alpha-1}\widehat{\widetilde{f}}(k,s). \end{aligned} \tag{5}$$

The inverse Laplace–Fourier transform of Eq. (5) yields

$$\frac{\partial^\alpha c(x,t)}{\partial t^\alpha} = d D_\theta^\beta c(x,t) + {}_0I_t f(x,t), \tag{6}$$

where

$$\begin{aligned} D_\theta^\beta f(x) = \frac{\Gamma(1+\beta)}{\pi}\Bigg\{ & \sin[(\beta+\theta)\pi/2]\int_0^\infty \frac{f(x+\xi)-f(x)}{\xi^{1+\beta}}\mathrm{d}\xi \\ & + \sin[(\beta-\theta)\pi/2]\int_0^\infty \frac{f(x-\xi)-f(x)}{\xi^{1+\beta}}\mathrm{d}\xi\Bigg\}. \end{aligned} \tag{7}$$

The Fourier transform of D_θ^β satisfies $\mathcal{F}\{D_\theta^\beta \varphi(x); k\} = -\eta_\theta^\beta(k)\widehat{\varphi}(k)$. $d = \sigma^\beta/\tau^\alpha$ and ${}_0I_t^{1-\alpha}$ is a fractional integral operator,[26] defined by

$${}_0I_t^{1-\alpha}\varphi(t) = \frac{1}{\Gamma(1-\alpha)}\int_0^t (t-t')^{-\alpha}\varphi(t')\mathrm{d}t'. \tag{8}$$

If $\beta = 2$, the Lévy diffusion operator (7) degrades into normal diffusion, whose diffusion operator is given by Δ and whose Fourier transform is $|k|^2$. For $0 < \beta < 2$, $\theta = 0$, the diffusion operator (7) can describe the symmetric Lévy diffusion of the particles, whose Fourier transform is given by $|k|^\beta$, which corresponds to the fractional diffusion operator Δ^β. So, the JLPD $\chi(x)$ we consider here is a more general distribution, including normal and fractional Laplace diffusion. Equation (6) is a general asymmetric anomalous diffusion model.

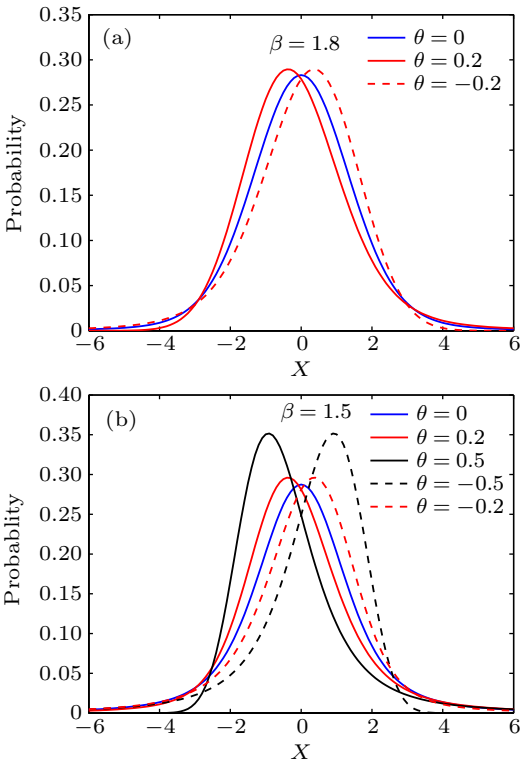


Fig. 2. The effect of skewness θ on the Lévy distribution with a fixed β: (a) with $\beta = 1.8$ and (b) with $\beta = 1.5$.

Since we mainly focus on how the asymmetry of Lévy diffusion affects Turing patterns, this paper will investigate the case of $\alpha = 1$ for the system (6), that is, the case of divergent variance of the JLPD, as follows:

$$\frac{\partial c(x,t)}{\partial t} = d D_\theta^\beta c(x,t) + f(x,t). \tag{9}$$

Usually, the first divergent moment of the WTPD can produce a fractional derivative with respect to time. For this case, in Ref. [28] we have shown that the fraction-derivative system can form spatial patterns even though its first-derivative counterpart cannot have spatial patterns.

3. The Brusselator model with asymmetric Lévy diffusion

3.1. General conditions for Turing and wave instabilities

In the previous section, we derived a generalized asymmetric Lévy diffusion system. Of course, this system can be expanded into the case of multiple kinds of reactants in two- or three-dimensional space. On the other hand, the Brusselator model is a well-known paradigm for studying Turing patterns.

Next, we will consider the Brusselator model with asymmetric Lévy diffusion as follows:

$$\frac{\partial u}{\partial t} = D_\theta^\beta u + a - (b+1)u + u^2 v, \tag{10a}$$

$$\frac{\partial v}{\partial t} = dD_\theta^\beta v + bu - u^2 v, \tag{10b}$$

where u and v denote the concentrations of activator and substrate, respectively. The parameter d is a diffusion rate that is scaled by the diffusion rate of u. Since we focus on spatial patterns regardless of boundary effects, the model (10) is equipped with a periodic boundary and the initial conditions are denoted as

$$u(x,0) = u_0(x), \quad v(x,0) = v_0(x).$$

This model has a spatially homogeneous steady state denoted by $E_* = (u_*, v_*)$ with

$$u_* = a, \quad v_* = \frac{b}{a}. \tag{11}$$

The model (10) without the Lévy diffusion term is a classical ODE system, and for this case the stability of E_* is determined by the following characteristic equation:

$$\lambda_0^2 - A_0\,\lambda_0 + D_0 = 0, \tag{12}$$

where

$$A_0 = b - 1 - a^2, \quad D_0 = a^2.$$

The ODE model corresponding to Eq. (10) at E_* is stable when $b < a^2 + 1$, and when $b > a^2 + 1$ periodic orbits appear.

In this section, we will discuss effect of the symmetry of the Lévy diffusion mechanism on pattern formation. First, we need to substitute the normal mode solution

$$\begin{pmatrix} u \\ v \end{pmatrix} = \begin{pmatrix} c_1 \\ c_2 \end{pmatrix} \exp(\lambda_k t + \mathrm{i}\boldsymbol{k}\cdot\boldsymbol{r}) \tag{13}$$

into Eq. (10), where λ_k is the growth rate of the perturbation in time t. $\boldsymbol{k}$ is its wave number and $\boldsymbol{r}$ presents a spatial position. Then one can obtain the following dispersion relation:

$$\lambda_k^2 - A_k\,\lambda_k + D_k = 0, \tag{14a}$$

where

$$A_k = -(1+d)\phi(k) + A_0, \tag{14b}$$

$$D_k = d\phi^2(k) + \phi(k)B_0 + D_0, \tag{14c}$$

$$B_0 = a^2 - d(b-1), \tag{14d}$$

$$\phi(k) = |k|^\beta \exp\left(\mathrm{i}(\mathrm{sign}(k))\theta\pi/2\right). \tag{14e}$$

This equation possesses complex coefficients, which is different from previous equations with real coefficients. Its eigenvalues can be given as

$$\lambda_k = \frac{A_k \pm \sqrt{A_k^2 - 4D_k}}{2}, \tag{15a}$$

where

$$\begin{aligned} A_k^2 - 4D_k \;=\; & (d-1)^2\phi^2(k) - 2\phi(k)[A_0(1+d) + 2B_0] \\ & + A_0^2 - 4D_0. \end{aligned} \tag{15b}$$

After some tedious calculations, the real and imaginary parts of the eigenvalue λ_k respectively read

$$\mathrm{Re}(\lambda_k) = \left[-(d+1)|k|^\beta \cos(\mu) + A_0 \pm \sqrt{R}\right] \Big/ 2, \tag{16a}$$

$$\mathrm{Im}(\lambda_k) = \left[-(d+1)|k|^\beta \sin(\mu) \pm \frac{2\sqrt{R}(R-P)}{Q}\right] \Big/ 2, \tag{16b}$$

where

$$\mu = \mathrm{sign}(k)\,\theta\pi/2, \tag{16c}$$

$$R = \left(P + \sqrt{P^2+Q^2}\right)/2, \tag{16d}$$

$$\begin{aligned} P \;=\; & (1-d)^2|k|^{2\beta}\cos(2\mu) - 2|k|^\beta\cos(\mu) \\ & \times [A_0(1+d) + 2B_0] + A_0^2 - 4D_0, \end{aligned} \tag{16e}$$

$$\begin{aligned} Q \;=\; & (1-d)^2|k|^{2\beta}\sin(2\mu) - 2|k|^\beta\sin(\mu) \\ & \times [A_0(1+d) + 2B_0]. \end{aligned} \tag{16f}$$

The occurrence of spatial patterns depends on the eigenvalue λ_k for which $\mathrm{Re}(\lambda_k) > 0$ for some $k > 0$. A critical value of a parameter is either diffusion parameters or otherwise, at which there is a quadratic tangency of the dispersion curve $\mathrm{Re}(\lambda_k) = 0$. This is a Turing or wave bifurcation depending on λ_k. In detail, if the eigenvalue λ_k is a real number for $k \in K$ and crosses zero from negative to positive as k changes in K, where K is a wavenumber set, then Turing instability occurs. If λ_k is a complex number, its real part changes from negative to positive, the imaginary part of λ_k, however, remains nonzero, and then wave instability occurs. Therefore, we can obtain a general condition of Turing or wave instability

$$A_0 + \sqrt{R} > (1+d)|k|^\beta \cos(\mu), \quad \text{for} \quad k \neq 0. \tag{17}$$

This is our first result. In particular, when $\theta = 0$ we can obtain a condition of Turing instability

$$\begin{cases} b < a^2 + 1, \\ d(b-1) - a^2 > 2a\sqrt{d}. \end{cases} \tag{18}$$

This can obtained from inequality (17) by tedious calculation. For $\theta \neq 0$, inequality (17) is the condition of wave instability if the imaginary part of λ_k is always nonzero. It is worth noticing that wave instability occurs in this two-component system equipped with asymmetric Lévy diffusion. This is different from the previous result in Refs. [7,27] that the minimal number of components for wave instability to occur is three.

3.2. Normal and fractional Laplace diffusions

In this section, we will give the theoretical and numerical results of the Turing patterns for the model (10). For numerical simulations, spatial discretization should first be considered. Throughout this paper, in one-dimensional space, we uniformly discretize the spatial region with length $L=8$ into $L=128$ lattices. For the two-dimensional case, the model (10) is restricted to a square region with side length $L=8$, and is discretized into a two-dimensional lattice with $L_x=128$ lattices in the horizontal direction and $L_y=128$ lattices in the vertical direction. We assume that the model (10) is equipped with a periodic boundary, and that its initial conditions are randomly taken as $u(x_i,t)=u_0+\xi_i^{(1)}$ and $v(x_i,t)=u_0+\xi_i^{(2)}$, where $\{\xi_i^{(j)}\}, i=1,2,\ldots,128, j=1,2$, follow a uniform distribution on $[0,1]$. After performing a fast Fourier transform for discrete space variables according to the spectral method for PDEs,[29] we obtain a group of ODEs, and then numerically calculate them by the Runge–Kutta method. Our programs are written in the Julia programming language.

Next, we first discuss two kinds of diffusion operators: normal and fractional Laplace diffusion operators. When $\beta=2$ and $\theta=0$, the Lévy diffusion operator D_0^2 turns into the Laplace operator Δ, i.e., the normal diffusion operator; for $0<\beta<2$ and $\theta=0$, the Lévy diffusion operator D_0^β becomes the fractional Laplace operator. For these two cases, their dispersion relations (14) can be written as

$$\lambda_k^2-[A_0-(1+d)k^\beta]\lambda_k+d|k|^{2\beta}+|k|^\beta B_0+D_0=0,\quad 0<\beta\le 2. \tag{19}$$

Model (10) with $\theta=0$ can undergo Turing and Hopf bifurcations depending on the real eigenvalues λ_k in Eq. (14). Here, we perform numerical simulations for λ_k with a bigger real part with the help of Eq. (16) with $a=4.5$ and $d=8$, since equation (14) has two eigenvalues. Let b be a control parameter of the Turing pattern for the system (10). $b_c=(1+a\sqrt{1/d})^2$ is the critical point for forming Turing patterns. Figure 3 shows the bigger real part of λ_k and its corresponding imaginary part with respect to the wave number k. When $\theta=0$, the eigenvalues are real numbers; otherwise they are imaginary numbers. For the case of $\theta=0$ and $b=6<b_c$, i.e., the diffusion operator is a symmetric normal or fractional Laplace operator, λ_k is a real number and less than zero for $k\neq 0$, implying that Turing patterns cannot appear. Taking the parameters $a=4.5$, $d=8$, $\beta=1.2$, $b=6$ and $\theta=0$, we plot the spatio–temporal trajectories of system (10) in one-dimensional space in Figs. 4(a) and 4(b), finding that the system (10) tends to the spatially homogeneous steady state E_*. In addition, when $b>b_c$, the system (10) with normal or fractional diffusion can produce spatial patterns with different phases and stripes for different bs, which were obtained in previous work.[23] Figure 6 illustrates the three different phases of the spatial patterns: stripes and hexagons. Furthermore, the Turing patterns of system (10) with fractional Laplace diffusion are implemented numerically for $b>b_c$,

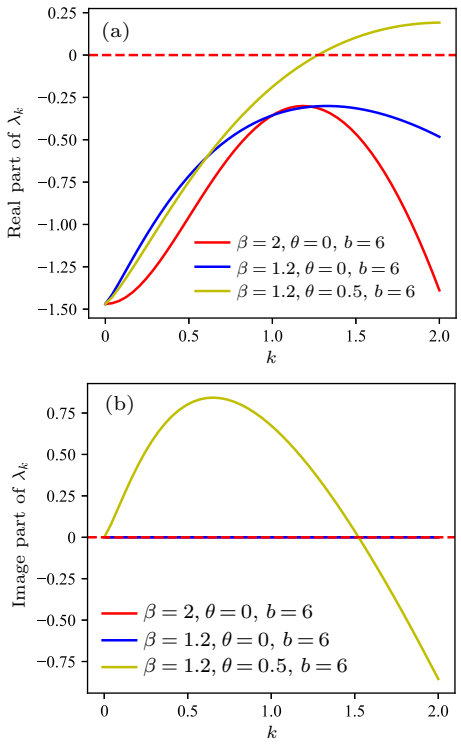


Fig. 3. The real (a) and imaginary (b) parts of λ_k in Eq. (7) versus the wavenumber k for the different parameters β, θ and b ($d=8$ and $a=4.5$).

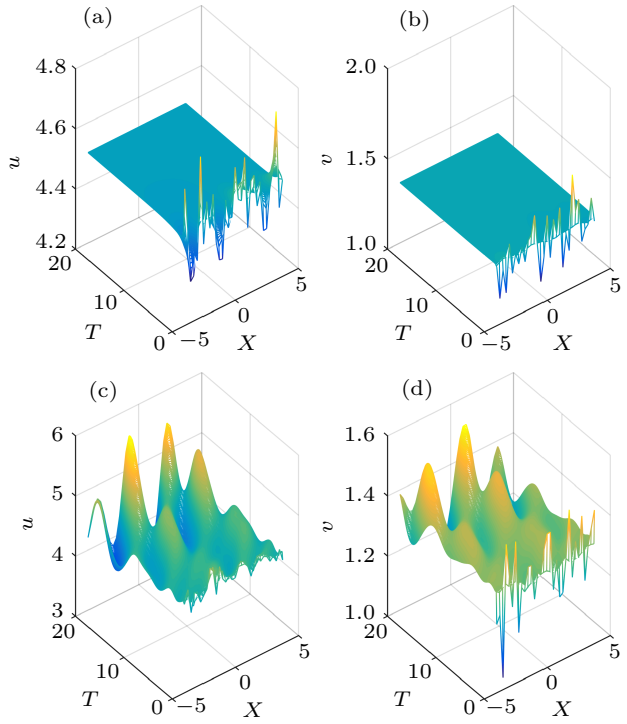


Fig. 4. Time evolution of model (10) with symmetric or asymmetric diffusion in one-dimensional space ($a=4.5$, $b=6$, $d=8$ and $\beta=1.2$). Panels (a) and (b) show the dynamical trajectories of u and v for $\theta=0$. The positive equilibrium $E_*=(4.5,1.33)$ is stable. Panels (c) and (d) show the dynamical trajectories of u and v for $\theta=0.5$.

with the finding that fractional Laplace diffusion can change the shape of the spatial patterns compared with those produced by the system (10) with normal diffusion. How fractional Laplace diffusion affects the patterns will be explored in the following subsection.

3.3. Asymmetric Lévy diffusion

Next we will uncover how the asymmetry of Lévy diffusion affects the stability of E^* for system (10). When $\theta \neq 0$, the eigenvalues λ_k in Eq. (14) are complex numbers according to Eq. (16). If one of these eigenvalues possesses a real part greater than zero then wave instability occurs for system (10) and wave patterns appear.

For the case of $\theta \neq 0$ (i.e., the diffusion operator is asymmetric), equation (19) can have at least one eigenvalue with a positive real part and non-zero imaginary part for $k \neq 0$ (see Fig. 3), implying that a wave pattern occurs. In Figs. 4(c) and 4(d), the system (10) with $\theta = 0.5$, in which the diffusion operator is asymmetric, are numerically implemented, showing that the system (10) finally evolves into a spatially heterogeneous steady state, i.e., wave patterns arise. These patterns are illustrated in Fig. 5. The subfigures on the first row in Fig. 5 show wave patterns for u and v in one-dimensional space. The subfigures on the second row show wave patterns in two-dimensional space. As a result, the asymmetry of Lévy diffusion can produce wave patterns, even though the system (10) equipped with normal or fractional Laplace diffusion cannot produce any spatial patterns in a certain parameter regime. This is our second main result.

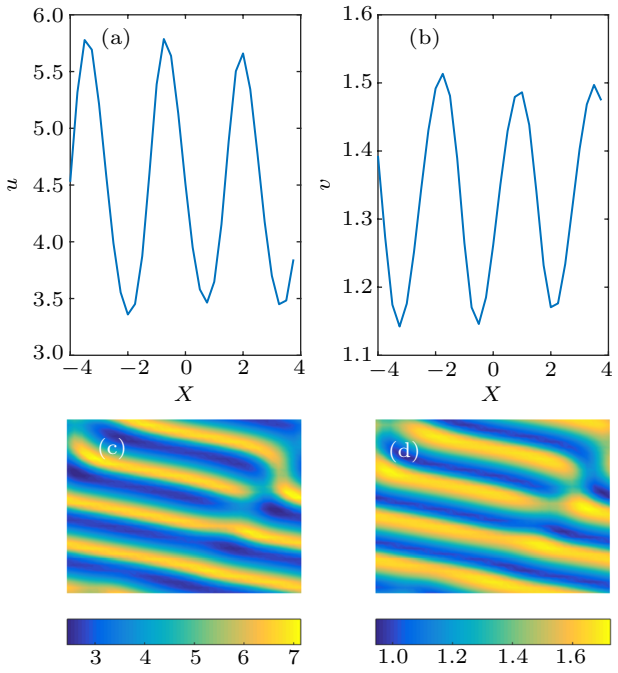


Fig. 5. The wave patterns of u and v. The wave patterns on the first row are performed in one-dimensional space. Those in the second row are their corresponding two-dimensional wave patterns ($a = 4.5$, $d = 8$, $b = 6$, $\theta = 0.5$ and $\beta = 1.2$).

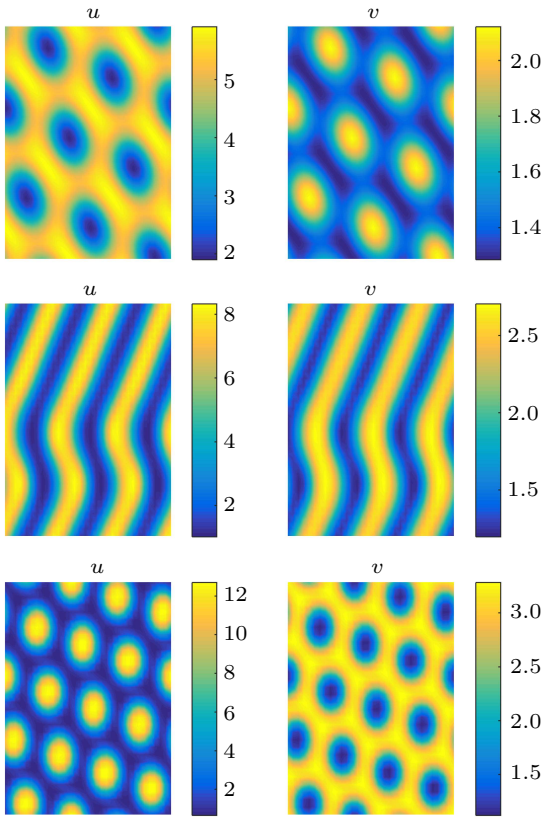


Fig. 6. Turing patterns of u and v for different parameters b: $b = 7$ for the subfigures on the first row, $b = 9$ for the subfigures on the second row and $b = 13.3$ for the subfigures on the third row ($\theta = 0$, $d = 8$ and $a = 4.5$).

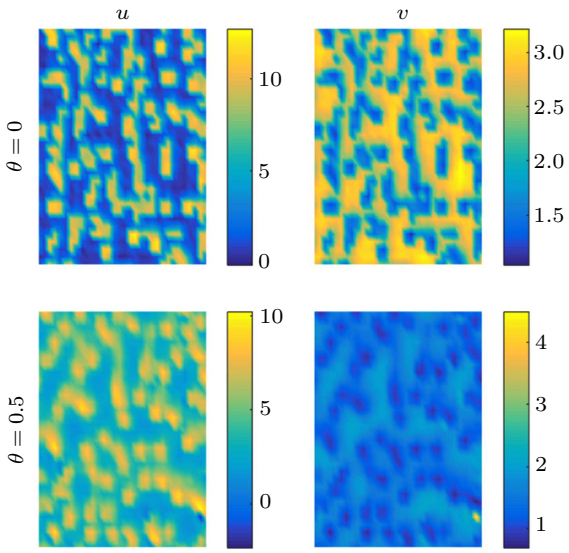


Fig. 7. Spatial patterns of the system (10) with $\beta = 1.2$, $b = 13.3$, $a = 4.5$ and $d = 8$. On the first row $\theta = 0$ and on the second row $\theta = 0.5$.

In Fig. 7, we numerically simulate the system (10) with fractional Laplace and asymmetric diffusion, respectively, finding that both fractional and asymmetric diffusion can change the phases of the spatial patterns compared with the patterns in the third row in Fig. 6. In order to uncover how fractional and asymmetric diffusion, respectively, affect the spatial patterns we now focus on the spatial patterns in one-

dimensional space, i.e., the system (10) is numerically calculated in one-dimensional space. In Fig. 8, panels (a) and (b) show the stationary spatial patterns of the system (10) with fractional Laplace diffusion in one-dimensional space; their corresponding power spectra are in panels (c) and (d), finding that fractional diffusion changes the phase and frequency of the spatial patterns but rarely the amplitude of the patterns. Figure 9 illustrates the power spectra of the spatial patterns arising from the system (10) with asymmetric Lévy diffusion, showing that the asymmetry factor can significantly change the amplitude and frequency of the spatial patterns. This is our third main result.

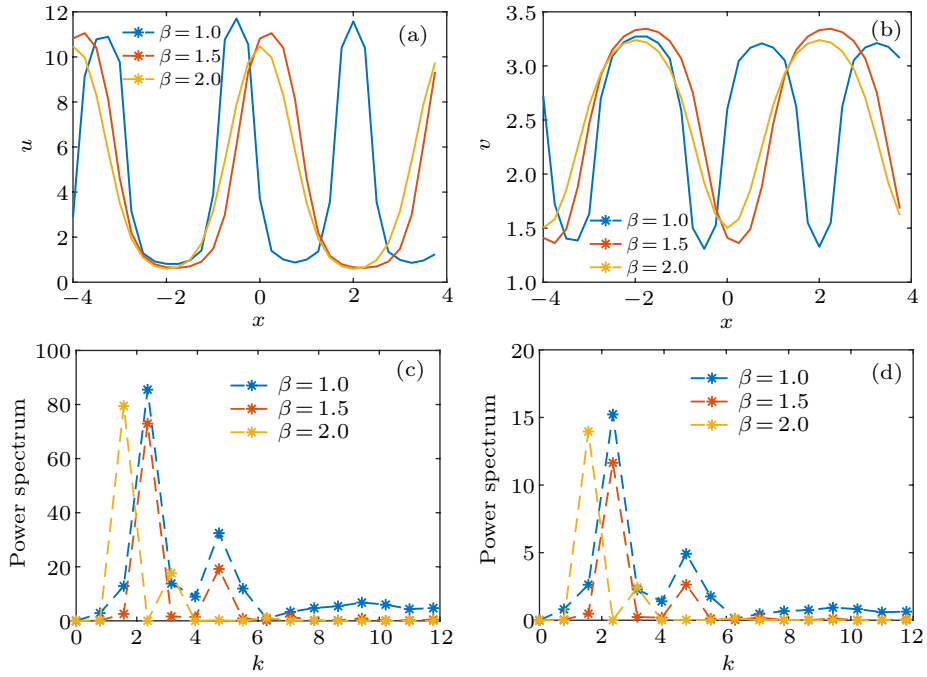


Fig. 8. One-dimensional patterns of the system (10) with symmetric Lévy diffusion ($b = 13.3$, $a = 4.5$, $d = 8$ and $\theta = 0$). Panels (a) and (b) show the one-dimensional patterns of u and v, respectively. Panels (c) and (d) are the power spectra of the patterns of u and v, respectively.

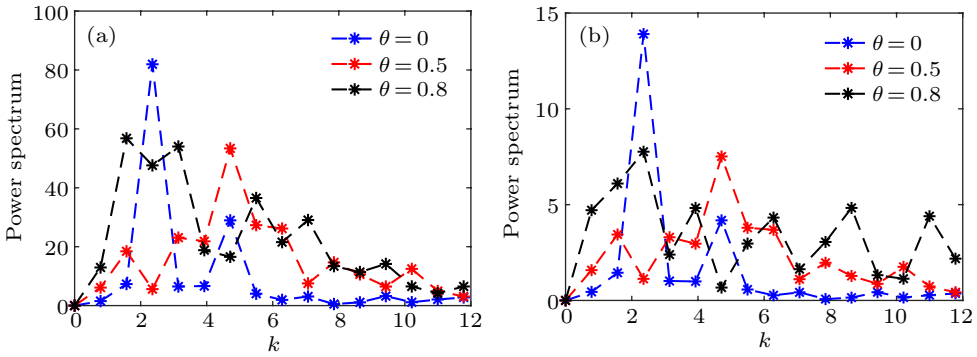


Fig. 9. The power spectrum of the one-dimensional spatial patterns coming from system (10) with asymmetric Lévy diffusion ($b = 13.3$, $a = 4.5$, $d = 8$ and $\beta = 1.2$). (a) The power spectra of u's patterns. (b) The power spectra of v's patterns.

4. Conclusion

Turing patterns have been researched for decades since the pioneering work of Alan Turing. Some researchers are still paying attention to spatial patterns. However, most current work assumes that the environments of reaction systems are uniform, so diffusion mechanisms, such as Gaussian diffusion, fractional Laplace diffusion and nonlinear diffusion,[22] are assumed to be symmetric in all space directions. However, the real environments of the systems are heterogeneous, often resulting in the diffusion mechanisms being different in each spatial direction, i.e., asymmetric. Up to now few papers, as far as we know, have studied this problem. Here, we apply the CTRW to build a generalized diffusive model with anomalous diffusion, including Gaussian diffusion (normal diffusion), symmetric fractional Laplace diffusion (symmetric Lévy diffusion) and asymmetric Lévy diffusion. In addition, we research the Brusselator model with asymmetric Lévy diffusion as an example as the Brusselator is a classical mathematical model and possesses rich dynamic behaviors. For this model we give the general condition for the formation of Turing and wave patterns, and find that the asymmetry of Lévy diffusion can produce wave patterns, even though

this model with normal and fractional Laplace diffusion cannot produce steady spatial patterns for certain parameters. The asymmetry of Lévy diffusion can significantly affect the amplitude and frequency of the spatial patterns. Our results are new and interesting, and enrich the currently known mechanisms of pattern formation.

In this paper, we mainly consider symmetric and asymmetric Lévy diffusion due to the divergence of the second moment of the particle's jumping length in one-step jumps. The divergence of the first moment of waiting time of a one-step jump leads to the generation of a time fractional derivative. This case has been set out in detail in our previous work.[28] However, we cannot research in depth the case when the first moment of the waiting time and the second moment of the jumping length diverge together (namely, the model in (6)). How its spatial patterns form is still an open problem, and will be studied in future work.

Acknowledgements

This work is supported by the National Natural Science Foundation of China (Grant Nos. 62066026, 62363027, and 12071408), PhD program of Entrepreneurship and Innovation of Jiangsu Province, Jiangsu University 'Blue Project', the Natural Science Foundation of Jiangxi Province (Grant No. 20224BAB202026), and the Science and Technology Research Project of Jiangxi Provincial Department of Education (Grant No. GJJ2203316).

References

[1] Turing A M 1952 *Phil. Tran. Roy. Soc. London B* **237** 37
[2] Tarnita C E, Bonachela J A, Sheffer E, Guyton J A, Coverdale T C, Long R A and Pringle R M 2017 *Nature* **541** 398
[3] Shoji H and Ohta T 2015 *Phys. Rev. E* **91** 032913
[4] Banerjee M and Banerjee S 2012 *Mathematical Biosciences* **236** 64
[5] Wang Y, Cao J, Sun G Q and Li J 2014 *Physica A* **412** 137
[6] Jacobo A and Hudspeth A J 2014 *Proc. Natl. Acad. Sci. USA* **111** 15444
[7] Korvasová K, Gaffney E A, Maini P K, Ferreira M A and Klika V 2015 *Journal of Theoretical Biology* **367** 286
[8] Hara N and Konishi K 2018 *Phys. Rev. E* **97** 052201
[9] Vetter R and Iber D 2020 *Nat. Commun.* **13** 1145
[10] Henry B I, Langlands T and Wearne S L 2006 *Phys. Rev. E* **74** 031116
[11] Carreras B A, Lynch V E and Del-Castillo-Negrete D 2003 *Phys. Rev. Lett.* **91** 018302
[12] Nec Y, Nepomnyashchy A A and Golovin A A 2008 *Europhys. Lett.* **82** 58003
[13] Golovin A A, Matkowsky B J and Volpert V A 2008 *SIAM Journal on Applied Mathematics* **69** 251
[14] Jia K, Hu L and Nie L 2024 *Chin. Phys. B* **33** 020502
[15] Gao J, Wang X, Liu X and Shen C 2023 *Chin. Phys. B* **32** 070503
[16] Zhang L and Tian C 2014 *Phys. Rev. E* **90** 062915
[17] Metzler R and Klafter J 2020 *Physics Reports* **339** 1
[18] Kutner R and Masoliver J 2017 *Euro. Phys. J. B* **90** 50
[19] Denisov S, Klafter J and Zaburdaev V 2015 *Rev. Mod. Phys.* **87** 483
[20] Yuste S B, Abad E and Lindenberg K 2010 *Phys. Rev. E* **82** 061123
[21] Fedotov S 2010 *Phys. Rev. E* **81** 011117
[22] Lombardo M C, Sammartino M, Sciacca V and Gambino G 2013 *Phys. Rev. E* **88** 042925
[23] Peña B and Pérez-García C 2001 *Phys. Rev. E* **64** 056213
[24] Schmiedeberg M, Stark H and Zaburdaev V 2008 *Phys. Rev. E* **78** 011119
[25] Mainardi F, Luchko Y and Pagnini G 2007 arXiv:cond-mat/0702419 [cond-mat.stat-mech]
[26] Mathai A M, Saxena R K and Haubold H J 2009 *The H-Function: Theory and Applications* (New York: Springer) p. 79
[27] Villar-Sepúlveda E and Champneys A R 2023 *Journal of Mathematical Biology* **86** 39
[28] Yin H and Wen X 2018 *Scientific Reports* **8** 5070
[29] Guo B 1998 *Spectral methods and their applications* (Singapore: World Scientific) p. 58